



Review

Optical spectroscopy and photodissociation dynamics of multiply charged ions

Ricardo B. Metz*

Department of Chemistry, University of Massachusetts, Lederle GRC, Amherst, MA 01003, USA

Received 17 March 2004; accepted 21 April 2004

Available online 28 May 2004

Abstract

Multiply charged ions are intriguing species whose reactivity and thermodynamic stability depends on the extent of ligation. The possibility of dissociating to two singly charged ions, which is often highly exothermic, leads to spectroscopy and dissociation dynamics that are qualitatively different from their singly charged counterparts. Various methods of producing multiply charged ions are discussed. Spectroscopy of small molecular dication, ligated/solvated transition metal dication, and multiply charged biological ions and metal cluster ions are discussed, with emphasis on our studies of d-d transitions in solvated transition metal dication, and the ensuing dissociation dynamics.

© 2004 Elsevier B.V. All rights reserved.

Keywords: Spectroscopy; Photodissociation; Dication; Electrospray**1. Introduction**

Although multiply charged molecular ions were first experimentally observed by Thomson in 1921 [1], the study of these energetic and highly reactive species has exploded over the past two decades. Fig. 1 shows schematic potentials for a ligated dication. Because the second ionization potential (IP) of even most metal atoms significantly exceeds the first IP of most stable molecules, small multiply charged ions are typically metastable with respect to dissociation into two singly charged ions. This process is termed charge reduction, charge separation, or Coulomb explosion. For small molecular ions charge reduction occurs by electron transfer. Depending on the ligands present, for larger ions charge reduction by proton or hydride transfer is usually more favorable than electron transfer; proton transfer dominates for protic ligands. Increasing the number of ligands stabilizes the multiply charged ion (Fig. 1b), and larger ions often dissociate by simply losing neutral ligands.

Transition metals in solution or in complexes typically have a nominal charge of +2 or +3. In the gas-phase, the charge on the metal center leads to much stronger

metal-ligand interactions than in singly charged ions. Spectroscopy of multiply charged metal containing ions in the gas-phase explores the strong noncovalent interactions that stabilize the charge. Varying the number and type of molecule bound to the metal reveals not only how the spectroscopic properties of the complex evolve from the isolated molecule to the bulk, but also shows interesting examples of small clusters with unique properties.

Much of the growth in spectroscopy of multiply charged ions is due to the development of ion sources with the high intensities required for spectroscopy. This has been coupled to sensitive spectroscopies, primarily based on detecting fragment ions produced by absorption and subsequent dissociation. Photofragment spectroscopy is also sensitive to the dissociation dynamics (kinetic energy release and anisotropy; lifetime). This is especially important as the possibility of dissociating to produce two like-charged ions, and the large Coulomb forces that this entails, means that the dissociation dynamics of multiply charged ions are very rich and are *qualitatively* different from those of singly charged ions or neutrals. Experimental techniques will be discussed, followed by a brief overview of studies of small molecular ions such as N_2^{2+} —very high-energy species that are often thermodynamically unstable by several electron volts, yet are kinetically stable and often have long-lived excited states. Studies of the spectroscopy and photodissociation

* Tel.: +1-413-545-6089; fax: +1-413-545-4490.

E-mail address: rbmetz@chemistry.umass.edu (R.B. Metz).

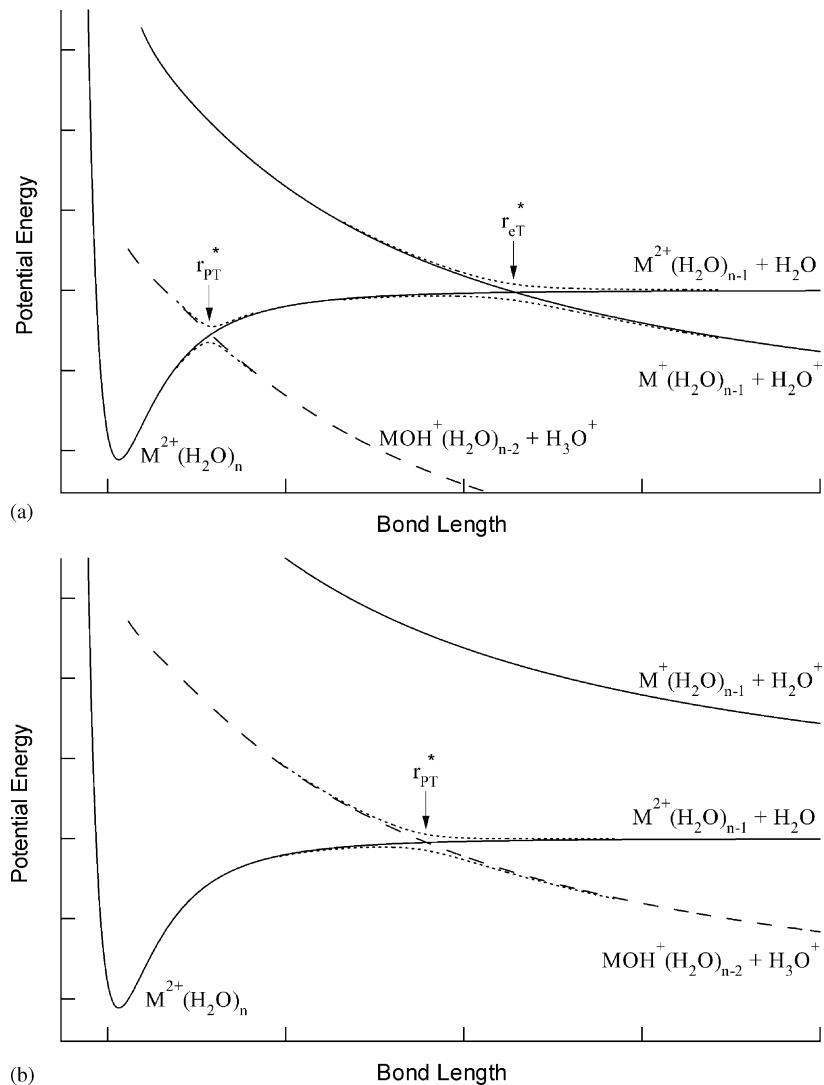


Fig. 1. (a) Schematic potentials for a solvated transition metal dication $M^{2+}(H_2O)_n$ showing the competition between dissociation by neutral loss, charge reduction through electron transfer (producing H_2O^+), and proton transfer (producing H_3O^+). Adiabatic potentials are shown with dotted lines; r_{eT}^* and r_{PT}^* are crossing points of diabatic curves for electron transfer and proton transfer, respectively. (b) As above, but for more highly solvated ion (larger n) or a metal with a smaller second ionization potential than in (a).

dynamics of solvated, multiply charged transition metal ions, including several examples from our lab, will be discussed in detail. For large molecules, the charge sites can be sufficiently separated that they do not interact strongly, and the reactivity and spectroscopy is not strongly dependent on the charge state. This class of molecules includes multiply charged biological ions and metal clusters, and their spectroscopy is presented in the last section.

In writing a review, there is always a tradeoff between breadth, depth, and manageable length. In focusing on the optical spectroscopy and dissociation dynamics of multiply charged ions we mention in passing several related fields that have recently been surveyed by others. A review by Duncan gives an excellent overview of the broader field of ion spectroscopy [2]. Reactions and collision induced dissociation of multiply charged ions have been studied extensively and are the subject of several reviews [3–7]. Also, a wide

variety of multiply charged negative ions have been studied using photoelectron spectroscopy, particularly by Wang and coworkers, who have characterized the repulsive Coulomb barrier that impedes photodetachment [7–10].

2. Experimental methods

2.1. Ion sources

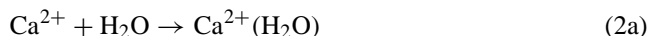
Multiply charged ions are challenging to make, and spectroscopy places greater demands on ion sources than simple mass spectrometry or collision induced dissociation. Many ions absorb weakly, or at wavelengths where intense light sources are not available, so it is useful to have sufficient ion currents to be able to detect dissociation products that are only 0.1–1% of the parent. The ion source should be

matched to the duty cycle of the light source. In addition, an ideal ion source would produce ions that are internally cold, which simplifies the spectroscopy. Due to these constraints, and the many types of multiply charged ions that have been studied, many different ion sources have been used. For spectroscopic studies, ligated, multiply charged ions have been produced by (a) further ionizing ligated neutrals or singly charged ions (pickup source/electron impact ionization); (b) adding ligands to smaller multiply charged ions (ablation source); or (c) desolvating solvated, ligated ions (electrospray).

While ligated *singly charged* ions are readily produced by termolecular reactions, Fig. 1a illustrates why this approach is difficult with multiply charged ions. If the second IP of the metal exceeds the first IP of the ligand, charge transfer often results:



The charge transfer is efficient when the curves cross at distances of $r_{eT}^* < 7 \text{ \AA}$ [4,11,12]. Even if electron transfer is endothermic, proton transfer reactions [13–15] often prevent the production of larger clusters:



as illustrated in Fig. 1b) (dashed curves). As a result, solvated, multiply charged ions are typically generated either by further ionizing existing clusters (so the ions are formed with $r < r_{PT}^*$) or by desolvating larger ions produced from solution.

Stace and coworkers have generated many gas-phase metal(II) complexes using a “pickup” source [16–19]. A mixture of ~1% of the ligand of interest seeded in argon expands through a pulsed nozzle. The neutral cluster beam then picks up metal atoms as it passes over a high-temperature effusion cell, which produces the metal vapor. The neutral metal-containing clusters are ionized by electron impact, which produces primarily singly charged ions, but gives sufficient yields of doubly charged ions for collision induced dissociation experiments and spectroscopy of strongly absorbing ions. Among the intriguing ions they have produced are $Cu^{2+}(Ar)$, $Ag^{2+}(Ar)$ and $Au^{2+}(Ar)$ [18]. In these ions, the second IP of the metal exceeds the first IP of the ligand by 4.5–5.8 eV. Ions in which the second IP of the metal exceeds the first IP of the ligand are often loosely called “unstable,” even if the ligated ion *may* be thermodynamically stable due to the strong metal–ligand interaction. They have also produced larger clusters, such as $Cu^{2+}(H_2O)_n$ ($n = 3–25$) [19]. The method is applicable to almost all metals, as only sufficient vapor pressure at the temperatures used is required. One notable advantage is that it is not limited to studying oxidation states that are stable in solution. Stace and coworkers have produced complexes with argon, water, ammonia and many organic compounds [16–19]; the primary constraint is that the ligand have

sufficient vapor pressure at room temperature. One disadvantage of the technique is that electron impact produces vibrationally excited ions. As they do not undergo further collisions, they can only cool by boiling off ligands. As a result, the cluster ions are not cold and have a nonthermal internal energy distribution.

In 1994, Velegrakis and Luder produced “stable” $Mg^{2+}(Ar)_n$ clusters, along with $Mg^{2+}(H_2O)(Ar)_n$, using a pulsed laser ablation source [20]. Recently, Duncan and coworkers [21] have used pulsed laser ablation to produce “unstable” ions such as $Mg^{2+}(CO_2)_n$, $Co^{2+}(Ar)_n$ and $Si^{2+}(Ar)_n$. They examined photodissociation of $Co^{2+}(Ar)$, which occurs primarily by electron transfer. They also produced $Mg^{2+}(H_2O)$ and $Co^{2+}(H_2O)$, but were not able to make larger hydrated clusters, presumably due to proton transfer reactions. Attempts to produce “unstable” complexes of Mg^{2+} with organic ligands such as acetonitrile, methanol and acetone were unsuccessful. They suggest that the multiply charged clusters are produced by electron impact or Penning ionization of neutral or singly charged clusters in the ablation source, so that when they are formed, the ions have $r < r_{PT}^*$ or $r < r_{eT}^*$ (Fig. 1) [20]. The ablation source shows great potential, as ions have many collisions with the carrier gas after they are produced, then expand into vacuum, resulting in substantial cooling. Also, the duty cycle of a pulsed laser ablation source is well matched to photofragment spectroscopy using pulsed lasers.

Electrospray mass spectrometry (ESI) was introduced by Yamashita and Fenn [22] in 1984, and a few years later Kebarle and coworkers [23,24] demonstrated that ESI gives excellent yields of solvated, multiply charged ions. Posey and coworkers have used ESI to produce solvated, ligated ions such as $Fe(bipy)_3^{2+}(CH_3OH)_n$ [25–27]. Electrospray is also the method of choice for producing multiply charged biological molecules. The mechanism of electrospray has been widely discussed [28–32].

The ability of electrospray to produce large, multiply charged ions makes it an ideal source for ion cyclotron resonance (ICR) spectrometers. An early study by Freiser and coworkers used laser ablation of a metal disk and ion-molecule reactions in the ICR to produce $LaC_2H_4^{2+}$ and $LaC_3H_6^{2+}$; they were subsequently dissociated using a lamp-monochromator combination [33]. However, ICR spectrometers are better suited to measuring low-resolution spectra of larger, more complex ions [34]. Multiply charged ions can be produced by electrospray, or more complex ions can be synthesized by subsequent ligand exchange or ion-molecule reactions in the ICR. The extremely high mass resolution is useful when dealing with heavy ions, and the long observation times aid in detecting slow dissociation of large ions near threshold [35]. This versatility comes at the expense of a low repetition rate, which is a disadvantage in measuring structured spectra, where dissociation must be measured at many different wavelengths.

Fig. 2 shows our second-generation electrospray photofragment spectrometer, which couples an electrospray

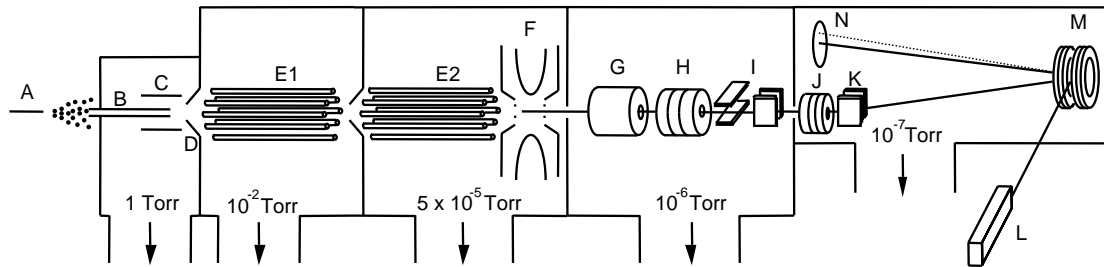


Fig. 2. Schematic of our electrospray time-of-flight photofragment spectrometer. Labels are described in the text.

source to time-of-flight mass analysis. An earlier version was used to study the spectroscopy of $\text{Ni}^{2+}(\text{H}_2\text{O})_n$ and $\text{Co}^{2+}(\text{H}_2\text{O})_n$ ($n = 4\text{--}7$) [36,37]. The electrospray source consists of a stainless steel hypodermic needle (A in Fig. 2) through which flows a 10^{-3} to 10^{-4} M solution of the appropriate metal(II) chloride in water. The needle is held at 7 kV relative to the desolvating tube (B), which acts as a counter electrode. The potential difference between the needle and counter electrode causes the production of micron-sized, highly charged droplets. Solvent evaporation causes the droplets to shrink, increasing the charge on the surface. Sufficiently small droplets fission, eventually producing small ions. The source operates at atmospheric pressure and can be purged with heated nitrogen to facilitate solvent evaporation. Clusters of M^{2+} with methanol, acetonitrile or DMSO are easier to produce than metal–water clusters: we use solutions in the desired solvent and operate at a lower needle voltage. Metal–ammonia clusters are produced by adding an ammonium salt to the solution [23,24]. Ions enter the interface chamber through the heated desolvation tube (B) [38] and are focused (C) through a skimmer (D). Producing good yields of the desired ion requires optimizing the temperature of the tube (40–70 °C) and the voltages on the tube, lens and skimmer. Low tube and skimmer voltages favor production of larger clusters such as $\text{M}^{2+}(\text{H}_2\text{O})_n$ ($n = 6\text{--}14$). Larger potential differences between the tube and skimmer lead to more energetic collisions of ions with the ~ 1 Torr gas in the interface chamber, which heats the ions, producing smaller clusters with $n \leq 6$. Even larger potential differences lead to extensive fragmentation and formation of $\text{MOH}^+(\text{H}_2\text{O})_n$ and $\text{H}^+(\text{H}_2\text{O})_n$. Electrospray produces ions with a nearly thermal internal energy distribution [27,39], although the temperature is slightly higher if higher potentials are used in the interface region and for more strongly bound ions, which have more difficulty cooling by solvent evaporation. Electrospray of metal(III) solutions with aprotic solvents can produce M^{3+} solvated by DMSO or acetonitrile [40]. The controversial ion $\text{Cu}^{2+}(\text{H}_2\text{O})$, which is thermodynamically unstable but has a lifetime of at least a microsecond is not observed directly in ESI, but has been produced by collision induced dissociation of larger ions and by high energy collisions of $\text{Cu}^+(\text{H}_2\text{O})$ [41]. Electrospray of solutions of ligated ions produces solvated, ligated ions (e.g., $\text{Fe}^{2+}(\text{bipy})_3(\text{CH}_3\text{OH})_n$

from methanolic tris(2,2'-bipyridyl)iron(II) perchlorate) [25]. Posey and coworkers have shown [26] that running under conditions that produce desolvated clusters ($n = 0$) and adding nitrogen saturated with another solvent to the source region leads to the production of $\text{Fe}^{2+}(\text{bipy})_3$ solvated by acetone, DMF, methanol, etc. This allows the synthesis of ions from solvents that do not spray well. In a similar vein, partial desolvation/resolvation in the interface region should allow the synthesis of ions such as $\text{M}^{2+}(\text{H}_2\text{O})_n(\text{benzene})_m$ from aqueous metal(II) solutions by adding benzene vapor to the electrospray source or directly to the interface region.

Electrospray produces a continuous ion beam, so it is logical to couple it to a continuous mass analyzer and CW lasers for spectroscopy. This is the approach used by Posey and coworkers in their studies of metal-to-ligand charge transfer (MLCT) bands in solvated, ligated ions such as $\text{Fe}^{2+}(\text{bipy})_3(\text{CH}_3\text{OH})_n$ [25–27]. Our work focuses on solvated ions such as $\text{M}^{2+}(\text{H}_2\text{O})_n$, whose visible absorption bands are due to metal centered d–d transitions. In octahedral $\text{M}^{2+}(\text{H}_2\text{O})_6$, these symmetry forbidden bands are about a factor of 1000 weaker than the MLCT transitions studied by Posey and coworkers, with maximum extinction coefficients of $\epsilon \approx 10 \text{ M}^{-1} \text{ cm}^{-1}$ ($\sigma \approx 1.7 \times 10^{-20} \text{ cm}^2$). We use pulsed dye lasers for our studies due to their superior fluence and tunability. We also use a pulsed (time-of-flight reflectron) mass spectrometer to mass select the parent ions and analyze charged fragments. A radiofrequency ion trap (F) couples [42,43] the continuous electrospray source to the pulsed mass spectrometer, which is limited to 20 Hz rep. rate by the laser. This approach is also used by Wang and coworkers to obtain photoelectron spectra of multiply charged anions produced by electrospray [9]. The continuous electrospray source leads to much higher gas loads than a pulsed ablation source and requires the use of several stages of differential pumping before the mass spectrometer. Octopoles (E1, E2) guide the ions through the differential chambers and into the ion trap, with minimal mass discrimination. Ions are trapped for up to 49 ms and thermalized to 300 K by approximately 1700 collisions with 1 mTorr helium and 100 collisions with 5×10^{-5} Torr background air. We will soon enclose the ion trap in a liquid–nitrogen cooled can and pre-cool the helium buffer gas. This will allow us to study ions at temperatures down to ~ 80 K [44,45]. Using an ion trap also allows us to synthesize new ions via ligand exchange reactions with

reagent gases leaked into the trap. Stored ions are extracted into the time-of-flight mass spectrometer by applying a 110 V pulse to the entrance plate of the trap. They are accelerated to 1800 V, re-referenced (G) to ground potential [46], focused by Einzel lenses (H and J) and steered (I) into the detector region. A pulsed mass gate (K) deflects the mass-selected cluster of interest into a reflectron (M).

2.2. Ion spectroscopy

The low number densities of ions makes absorption and emission spectroscopies very challenging, and this is especially true of multiply charged ions. So, spectra are typically obtained using indirect methods of detecting absorption—monitoring the appearance of product ions or parent ion depletion following irradiation of a mass selected ion beam [47]. Product ions are usually formed by photodissociation (often accompanied by charge transfer), but irradiation can lead to further ionization of large ions [48]. In our photofragment spectrometer, ions are excited at the turning point of the reflectron using the unfocused output of a Nd:YAG-pumped dye laser (L). With frequency doubling and mixing, the laser system is tunable from 220 to 850 nm. Parent and fragment ions are detected by 40 mm dia. dual microchannel plates (N). The resulting signal is collected on a 500 MHz digital oscilloscope and the masses of parent and fragment ions are determined by their flight times. We make two types of measurements. *Difference spectra* are the difference between time-of-flight spectra obtained with the dissociation laser blocked and unblocked at a fixed wavelength. They identify fragment channels and branching ratios. The shapes of fragment peaks reflect the kinetic energy release, anisotropy, and dissociation rate [36,37,49,50]. The *photodissociation spectrum* of an ion is obtained by monitoring the yield of a specific fragment ion as a function of wavelength and normalizing to parent intensity and laser fluence. It is the absorption spectra of those ions that dissociate to form the fragment being monitored. If absorption of light always leads to photodissociation, then the photodissociation spectrum of a molecule mirrors its absorption spectrum. This is expected to be the case for many ligated, multiply charged ions, where ligand loss provides a facile dissociation pathway. For example, loss of one water from $\text{Co}^{2+}(\text{H}_2\text{O})_6$ requires only $\sim 8000 \text{ cm}^{-1}$ and $15,500\text{--}22,000 \text{ cm}^{-1}$ photons lead to rapid photodissociation of $\text{Co}^{2+}(\text{H}_2\text{O})_6$ by loss of one or two water molecules [37]. Again, lack of tailing in the time-of-flight profile (indicating rapid, $<50 \text{ ns}$, dissociation) and loss of multiple solvent molecules are a strong indication that absorption leads to dissociation in this system.

3. Optical spectroscopy of multiply charged ions

3.1. Small molecular ions

Due to their interesting bonding and dissociation properties and importance in plasmas, several groups have studied

the spectroscopy of multiply charged molecular ions. Recent reviews have dealt with high resolution (rotationally resolved) spectroscopy of diatomic dications [51] and with the reactions and spectroscopy of larger multiply charged ions [5,52], so these ions will only be briefly discussed. Although the ground state of N_2^{2+} lies 4.4 eV above $\text{N}^+ + \text{N}^+$, several electronic states of N_2^{2+} are quasi-bound, supporting several vibrational levels at short bond length [53,54]. Many of these states have been characterized from rotationally resolved emission [55–57] and ion beam photodissociation spectra [47,54,58,59]. Rotationally resolved spectra have also been obtained for NO^{2+} by emission [60,61], but photodissociation spectra are unstructured [51,62]. In DCl^{2+} , vibrational excitation of the long-lived $v = 1$ state to the short-lived $v = 2$ state produces $\text{D}^+ + \text{Cl}^+$ with 4.9–6 eV kinetic energy release. The vibrational spectrum shows vibrational and even hyperfine structure, and the measured widths of individual lines are in good agreement with calculations [51,63,64].

Photodissociation of larger molecular ions leads to richer dynamics, with competition between charge reduction and loss of neutral fragments. Unfortunately, electronic transitions tend to be to repulsive states, leading to unstructured spectra [52]. Thus, for example, photolysis of SiF_2^{2+} leads to charge reduction, but the major channel is F atom loss to produce SiF^{2+} , especially at higher energies; Si^{2+} is also observed above 2.2 eV [65]. Competition between neutral loss and charge separation is also observed in photolysis of CCl_3^{2+} , CF_3^{2+} , SF_3^{2+} and SF_2^{2+} [66,67], and is a recurring theme in photolysis of ligated transition metal ions as well.

3.2. Ligated transition metal ions

With the development of pickup and, especially, electrospray sources, several groups have studied transition metal complexes in the gas-phase, examining the properties of ions in which the metal is in its “normal” oxidation state of +2 or +3. While complexes with charged ligands don’t require the study of multiply charged ions [68], most studies have focused on neutral ligands. Several of these studies use gas-phase techniques to address classic issues in inorganic chemistry. How do the geometry and electronic states of a transition metal complex depend on the number and type of ligands? How does the solvent stabilize the complex and affect its spectroscopy?

Studying the spectroscopy of size-selected cluster ions allows control over the number and type of molecule bound to the metal center, or solvating a ligated ion. Gas-phase studies also allow the investigation of coordinatively unsaturated complexes which are unstable in solution. In addition to the spectroscopic studies discussed below, there is a large body of work on reactions and collision induced dissociation of solvated and ligated multiply charged transition metal ions [23,24,69–77].

3.2.1. Metal-to-ligand charge transfer spectra of ligated complexes

In 1996, Posey and coworkers found that $M(\text{bpy})_3^{2+}(\text{CH}_3\text{OH})_n$ ($M = \text{Fe}, \text{Ru}$) have metal-to-ligand charge transfer (MLCT) bands that are similar to those found in solution [25], demonstrating that electrospray can be used to produce gas-phase transition metal complexes which retain the oxidation state of the metal. They have gone on to study the effect of the number and type of solvent molecules on MLCT transitions in Fe^{2+} and Ru^{2+} ligated by bipyridine and terpyridine (terpy) [25–27,78–80]. Fig. 3 shows the evolution of the photodissociation spectra of $\text{Fe}(\text{terpy})_2^{2+}(\text{DMSO})_n$ with increasing solvation. As the photon energy greatly exceeds the solvent binding energy, the photodissociation spectra should be equivalent to the absorption spectra of the clusters. The shift in the absorption maximum reflects the contributions of successive solvent molecules to the solvent reorganization energy which accompanies charge

transfer. By modeling how the maximum depends on the number of solvent molecules they showed that over half the solvent reorganization energy in the MLCT transition is due to solvent molecules in the first shell [79]. Complexes with different solvent molecules can be conveniently synthesized by spraying methanolic solutions of $\text{Fe}(\text{terpy})_2^{2+}$ in an atmosphere saturated with the solvent of interest (see Section 2.1 and [26]). These studies showed that a dielectric continuum model predicts the shift in the absorption maximum with solvents of differing polarity surprisingly well, even for clusters with as few as four solvent molecules [78].

Stace and coworkers have studied metal-to-ligand charge transfer and d-d transitions in $\text{Ag}^{2+}(\text{pyridine})_n$ and $\text{Cu}^{2+}(\text{pyridine})_n$ ($n = 2–7$) in the visible [81,82] and UV [83]. In the visible, the photodissociation spectrum of $\text{Cu}^{2+}(\text{pyridine})_4$ is similar to that of $\text{Cu}(\text{II})/\text{pyridine}$ complexes in solution, but the gas-phase spectra shift to the red for larger clusters (Fig. 4), while the solution spectra shift to the blue. The intensity of the transition ($\varepsilon_{600\text{ nm}} \approx 100 \text{ M}^{-1} \text{ cm}^{-1}$) is reasonable for a d-d transition [81,82].

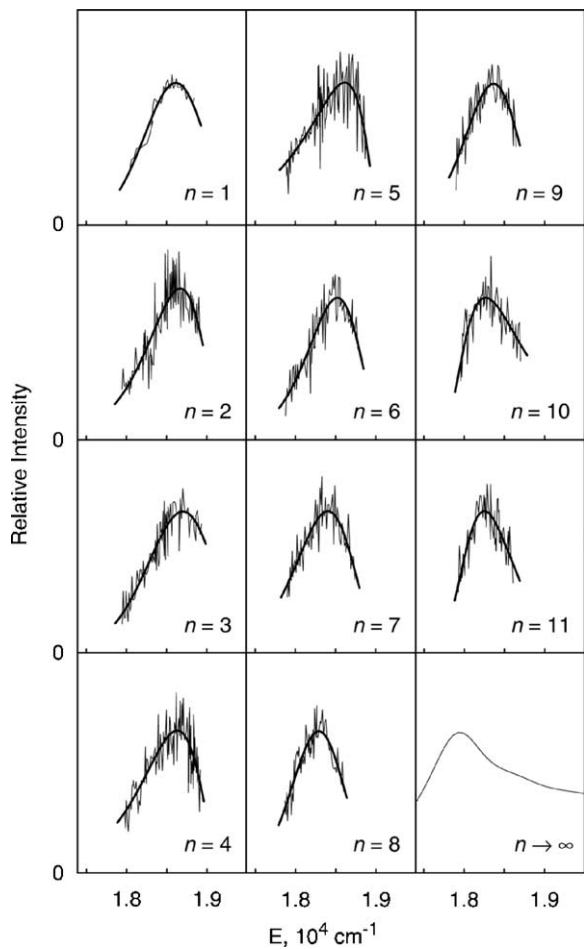


Fig. 3. Photodissociation spectra of $\text{Fe}(\text{terpy})_2^{2+}(\text{DMSO})_n$ ($n = 1–11$) obtained at photon energies in the range $17,800–18,900 \text{ cm}^{-1}$. The spectrum shown for $n = 3$ corresponds to $\text{Fe}(\text{terpy})_2^{2+}(\text{DMSO}-\text{d}_6)_3$. The smooth lines through the data represent nonlinear least-squares fits to log-normal functions. The absorption spectrum of $[\text{Fe}(\text{terpy})_2](\text{PF}_6)_2$ in DMSO solution is designated by $n \rightarrow \infty$. Reprinted with permission from [79]. Copyright 1998 American Chemical Society.

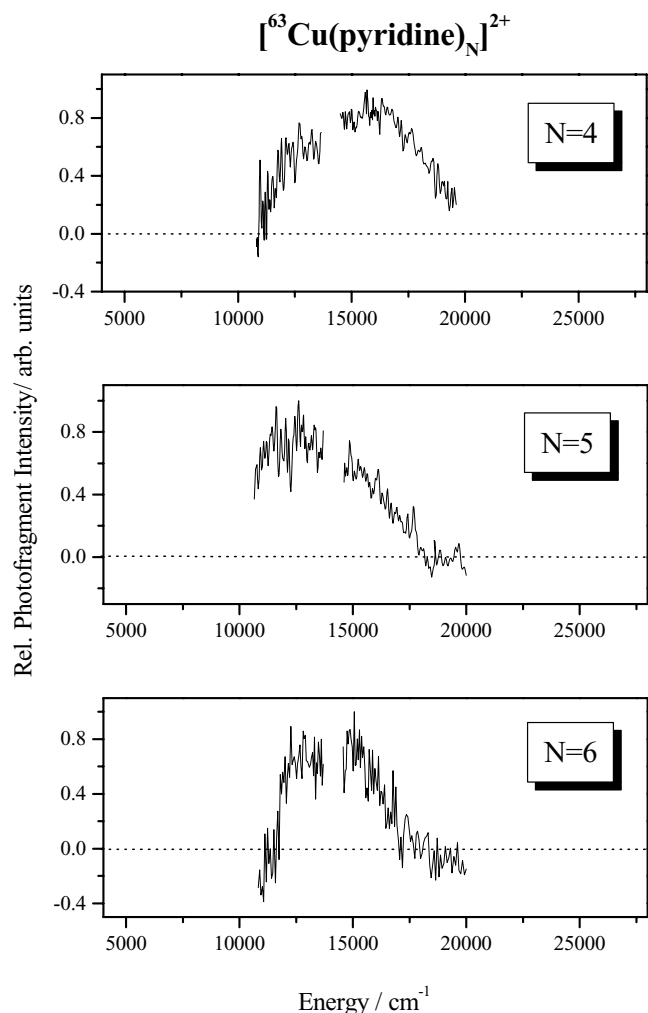


Fig. 4. Photodissociation spectra of $\text{Cu}^{2+}(\text{pyridine})_n$, with $n = 4–6$. Reproduced with permission from The Royal Society of Chemistry from [82].

Dissociation in the visible and UV occurs by simple ligand loss, with larger clusters tending to lose more ligands. Surprisingly, the corresponding Ag^{2+} clusters behave somewhat differently. Although larger clusters ($n = 6$) dissociate by ligand loss, small clusters undergo electron transfer to form pyridine $^+$ and $\text{Ag}^+(\text{pyridine})_m$. The visible band of $\text{Ag}^{2+}(\text{pyridine})_4$ is somewhat more intense than that of the copper complex ($\epsilon \approx 500 \text{ M}^{-1} \text{ cm}^{-1}$), implying that the transition has significant charge transfer character [81,82]. This revises the traditional assignment (from solution studies) of the visible band of this complex to a d-d transition.

Electrospraying solutions of complexes of transition metals with negatively charged ligands leads to multiply charged negative ions. Most studies of multiply charged negative ions are by photodetachment photoelectron spectroscopy and are discussed in detail elsewhere [7–10]. In a very thorough study, Kappes and coworkers looked at photodissociation of IrBr_6^{2-} and IrCl_6^{2-} from 1.5 to 2.9 eV photon energy [84]. Primary photodissociation of IrBr_6^{2-} leads to $\text{IrBr}_5^- + \text{Br}^-$, with 2.2 ± 0.2 eV kinetic energy release. The photodissociation spectra are similar to absorption spectra of the complexes in aqueous solution, with a slight shift to lower energy for some peaks. These charge-transfer bands are fairly intense, with photodissociation cross-sections of $\sigma \approx 1\text{--}3.5 \times 10^{-17} \text{ cm}^2$.

3.2.2. Metal-based d-d transitions

In aqueous solution, first-row transition metal M^{2+} are surrounded by an inner solvation shell of six water molecules, which leads to an octahedral, or nearly octahedral, $\text{M}^{2+}(\text{H}_2\text{O})_6$ species [85]. Crystal field theory states that the resulting field splits the degenerate atomic 3d orbitals into molecular e_g and t_{2g} orbitals. The absorption bands that give aqueous solutions of M^{2+} their characteristic colors have traditionally been assigned to transitions between these molecular orbitals. These transitions are weak, with typical extinction coefficients $\epsilon \approx 1\text{--}10 \text{ M}^{-1} \text{ cm}^{-1}$ [86,87]. Because d-d transitions are symmetry forbidden for M^{2+} in octahedral complexes (or any structure containing a center of inversion), the observation of these transitions is usually attributed to vibronic coupling [86–88]. This view was questioned by a high-level ab initio study of the electronic spectroscopy of $\text{Co}^{2+}(\text{H}_2\text{O})_n$ ($n = 4\text{--}6$) complexes by Gilson and Krauss [89]. They calculated the energies and intensities for transitions to the first ten electronic states for these ions. They find that the Jahn-Teller distortion for $\text{Co}^{2+}(\text{H}_2\text{O})_6$ is very small and the oscillator strength (f) for $\text{Co}^{2+}(\text{H}_2\text{O})_6$ transitions in the visible is zero. The oscillator strength remains very low ($f \leq 10^{-6}$), even when the complex is distorted by moving an axial water 0.15 Å. This is inconsistent with the experimental observation that the aqueous Co^{2+} (${}^4\text{T}_{1g}(\text{P}) \leftarrow {}^4\text{T}_{1g}(\text{F})$) absorption band near 510 nm has $f \approx 8 \times 10^{-5}$ if $\text{Co}^{2+}(\text{H}_2\text{O})_6$ is assumed to be the chromophore. Their provocative conclusion is that the aqueous absorption spectrum is due to a strongly-absorbing minor species, probably the $n = 5$ cluster, with the $n = 4$

structure contributing at high temperature [89,90]. This view has been challenged by Swaddle and coworkers, who measured absorption spectra of aqueous cobalt(II) at temperatures up to 625 K and found that the major absorption peak changed little with temperature [91,92]. They do observe a new absorption band that grows in at higher temperatures and assign it to the $n = 4$ complex.

We undertook to address the controversy directly, by measuring the spectra of isolated $\text{Co}^{2+}(\text{H}_2\text{O})_n$ ($n = 4\text{--}6$) ions in the gas-phase. By studying mass-selected ions, the spectroscopy of each particular sized cluster can be measured, free from interference from surrounding solvent molecules. In addition, coordinatively unsaturated complexes that are difficult to prepare in the condensed phase can be made and spectroscopically characterized in the gas-phase. This allows us to measure how the d-d bands evolve with coordination number, without changing the ligand. Fig. 5 compares the photodissociation spectrum of $\text{Co}^{2+}(\text{H}_2\text{O})_6$ to the absorption spectrum of aqueous cobalt(II). The photodissociation spectrum mirrors the absorption spectrum as excited ions readily dissociate by loss of one or two H_2O molecules (loss of one H_2O requires $\sim 8000 \text{ cm}^{-1}$ [73]). The cluster spectrum is very similar to that of the solution, but is shifted $\sim 1500 \text{ cm}^{-1}$ to lower energy. The maximum photodissociation cross-section of the cluster is $\sigma \approx 6 \times 10^{-20} \text{ cm}^2$, which corresponds to an extinction coefficient $\epsilon \approx 37 \text{ M}^{-1} \text{ cm}^{-1}$. Uncertainties in the absolute cross-section are estimated at 50% and are due to laser beam nonuniformity and uncertainty in the overlap between the laser and ion beams [37,93]. The spectrum of $\text{Co}^{2+}(\text{H}_2\text{O})_7$ is similar, but is only shifted by 1350 cm^{-1} [37]. We were unable to photodissociate the $n = 5$ cluster, although it is predicted [89] to absorb in the same wavelength region as the $n = 4$ and 6 clusters, so it does not appear to absorb significantly more strongly than $\text{Co}^{2+}(\text{H}_2\text{O})_6$. These results (and similar results on $\text{Ni}^{2+}(\text{H}_2\text{O})_n$ ($n = 4\text{--}7$) [36]) completely support the traditional view: $\text{Co}^{2+}(\text{H}_2\text{O})_6$ is the chromophore responsible for the characteristic absorption spectrum of cobalt(II) solutions.

So, why do the calculations underestimate the intensity of the transitions? Gilson and Krauss estimated the effect of vibronic coupling on the spectrum of $\text{Co}^{2+}(\text{H}_2\text{O})_6$ by moving one water ligand 0.15 Å from the metal. They found that the distorted complex still had a very low transition probability ($f < 10^{-6}$) [89]. Vibronic coupling in small symmetric molecules such as CO_2 , formaldehyde and, especially, benzene have been the subject of several theoretical studies [94–96]. Typically, these studies involve calculating electronic transition intensities for complexes distorted along each vibrational normal mode with the correct symmetry to allow vibronic coupling. In benzene, transitions to the lowest excited state (${}^1\text{B}_{2u}$) from the ${}^1\text{A}_{1g}$ ground state are forbidden by symmetry. Although four vibrations in benzene have the correct symmetry to make the transition vibronically allowed, 90% of the electronic transition intensity is due to a single vibration—the in-plane ring deformation

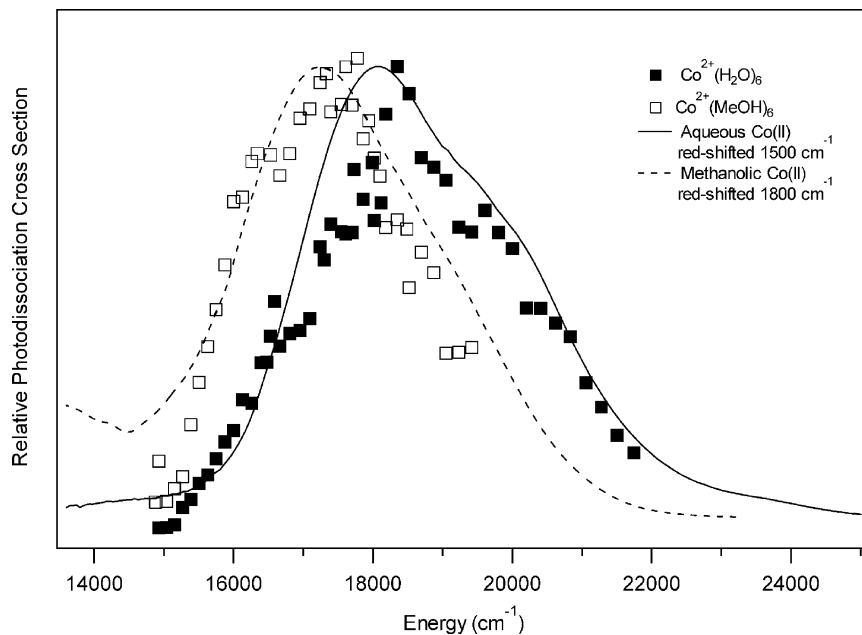
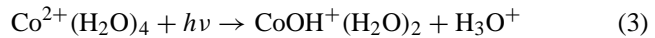


Fig. 5. Photodissociation spectra of gas-phase $\text{Co}^{2+}(\text{H}_2\text{O})_6$ and $\text{Co}^{2+}(\text{MeOH})_6$. The absorption spectra of cobalt(II) in water and methanol solution are also shown, shifted to facilitate comparison. Each spectrum has been normalized to a relative intensity of 1.

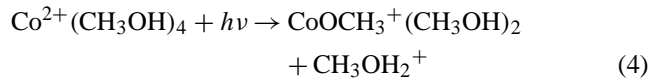
(v_6) [96]. In the case of $\text{Co}^{2+}(\text{H}_2\text{O})_6$, the d–d bands are vibronically allowed with a contribution from a vibration with *ungerade* symmetry. As there are 27 such vibrations, treating vibronic coupling properly is very computationally demanding. The approach used by Gilson and Krauss of stretching one metal–ligand bond corresponds to a combination of normal modes and does not include the effect of, for example, ligand–metal–ligand bending on the electronic transition. In order to try to identify the specific vibrations responsible for the observed intensity in the visible bands of $\text{Co}^{2+}(\text{H}_2\text{O})_6$ we are calculating vibronic coupling using time-dependent density functional theory (TD-DFT) with the B3LYP hybrid density functional. TD-DFT is much less computationally demanding than the methods used by Gilson and Krauss, but is surprisingly accurate for electronic transitions in transition-metal containing ions [97,98]. Preliminary results give a calculated integrated absorption of $f \approx 4 \times 10^{-5}$, in good agreement with the experimental solution value $f \approx 8 \times 10^{-5}$, and most of the vibronic intensity is due to a handful of vibrations.

Swaddle and Fabes observed a new absorption in aqueous cobalt(II) at high temperature and assigned the absorption to aqueous $\text{Co}^{2+}(\text{H}_2\text{O})_4$ [91]. The photodissociation spectrum of the isolated $\text{Co}^{2+}(\text{H}_2\text{O})_4$ ion confirms this assignment (Fig. 6). The spectrum of the gas-phase ion is slightly narrower, presumably due to the absence of inhomogeneous broadening and the lower temperature ($\sim 300\text{ K}$ versus 497 K). The $n = 4$ complex absorbs significantly more strongly ($\sigma \approx 2.5 \times 10^{-19}\text{ cm}^2$) than the $n = 6$ cluster. This is expected for a tetrahedral complex, as it lacks a center of inversion. As a result, contributions of metal-based p orbitals to the bonding add some allowed d–p character to

the forbidden d–d transition [86,87]. Although larger clusters dissociate by simple water loss, the $n = 4$ complex undergoes proton transfer:



As a result of Coulomb repulsion between the fragment ions, dissociation leads to substantial kinetic energy release. Fig. 7 shows the time-of-flight profile of the H_3O^+ fragment. Ions that dissociate towards and away from the detector arrive at early and late times, respectively; ions that dissociate perpendicular to the flight path miss the detector, causing the dip in the center of the spectrum. The 110 kJ/mol kinetic energy release (KER) is 48% of the available energy (much higher KERs have been observed for small molecular ions, see Section 3.1). The analogous methanol complex also dissociates via proton transfer:



The time-of-flight profile (Fig. 7) indicates a slightly higher KER. Tailing in the spectrum indicates that $\text{Co}^{2+}(\text{CH}_3\text{OH})_4$ photodissociates on a 200 ns time scale; we observe no tailing for $\text{Co}^{2+}(\text{H}_2\text{O})_4$, indicating a lifetime below 30 ns .

The relatively low kinetic energy release suggests that the positive charges are well separated at the transition state for proton transfer. This is consistent with B3LYP calculations by Beyer that predict a salt-bridge mechanism in which one of the four inner-shell waters moves to the outer shell, then abstracts a proton (leading to a salt-bridge arrangement $\text{M}^{2+} \cdots \text{OH}^- \cdots \text{H}_3\text{O}^+$) and departs [50]. Fig. 8 shows the calculated potential, along with structures of transition states

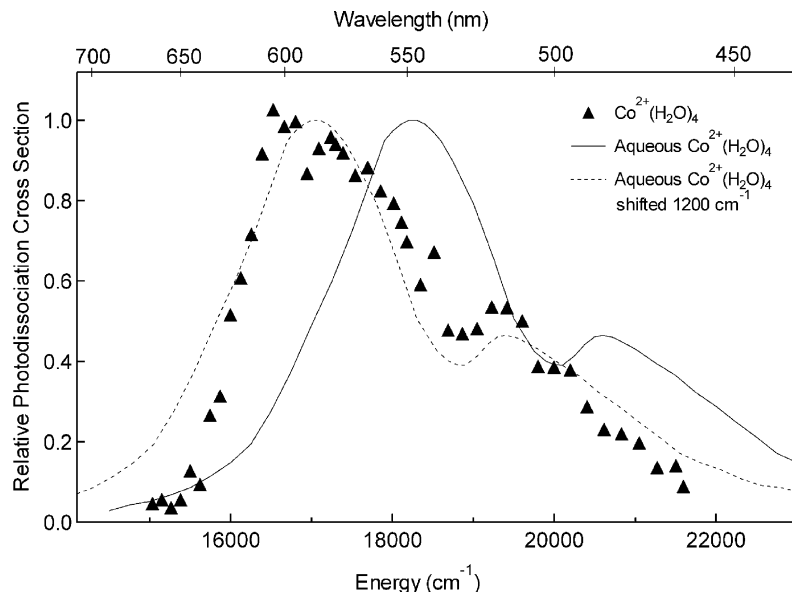


Fig. 6. Comparison of the photodissociation spectrum of $\text{Co}^{2+}(\text{H}_2\text{O})_4$ (triangles) and the spectrum assigned to aqueous $\text{Co}^{2+}(\text{H}_2\text{O})_4$ at 497 K by Swaddle and Fabbes [91] (solid line). Also shown is the aqueous spectrum shifted 1200 cm^{-1} to lower energy.

and local minima. This is the quantitative version of the proton transfer channel shown schematically in Fig. 1b. This mechanism also suggests that $\text{Co}^{2+}(\text{CH}_3\text{OH})_4$ dissociates more slowly because the additional vibrational degrees of freedom lead to a much higher density of states near the transition state. The higher kinetic energy release observed

for the methanol complex suggests that it may have a higher barrier to dissociation than the hydrated complex; this would also contribute to lowering the dissociation rate.

Although these studies are still in their infancy and we have looked at few systems, we have already found an ion in which the small size of the complex and absence of solvent

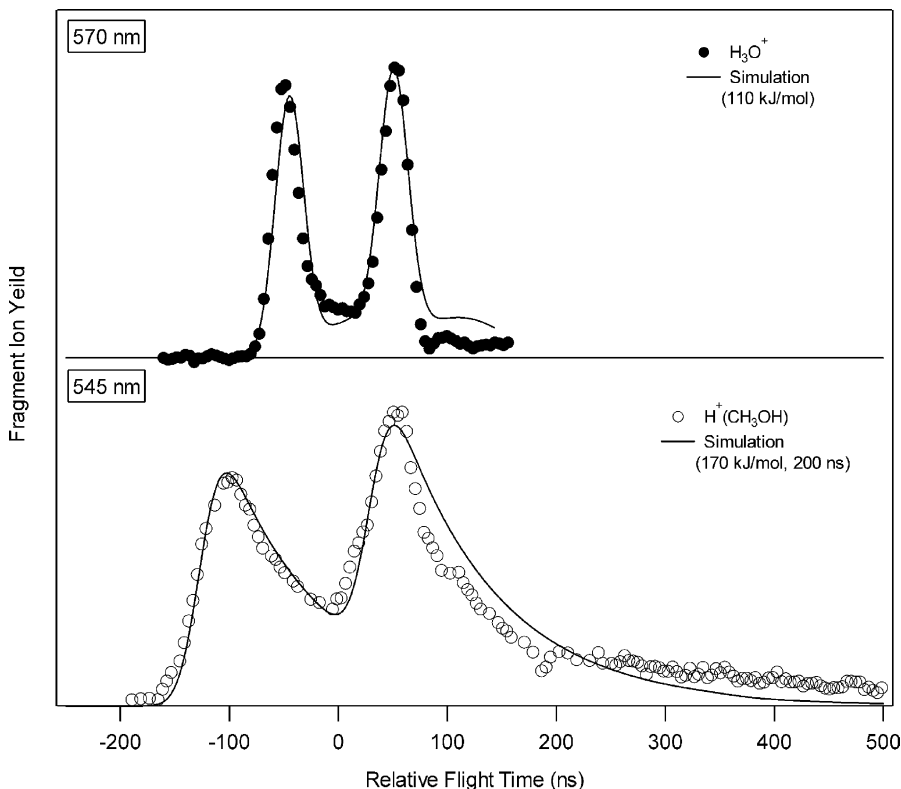


Fig. 7. Time-of-flight spectra of H_3O^+ and $\text{H}^+(\text{CH}_3\text{OH})$ produced by photodissociation of $\text{Co}^{2+}(\text{H}_2\text{O})_4$ and $\text{Co}^{2+}(\text{CH}_3\text{OH})_4$, respectively. The solid lines are a simulation of the time-of-flight profile with a single kinetic energy release and, for $\text{Co}^{2+}(\text{CH}_3\text{OH})_4$, a dissociation lifetime of 200 ns.

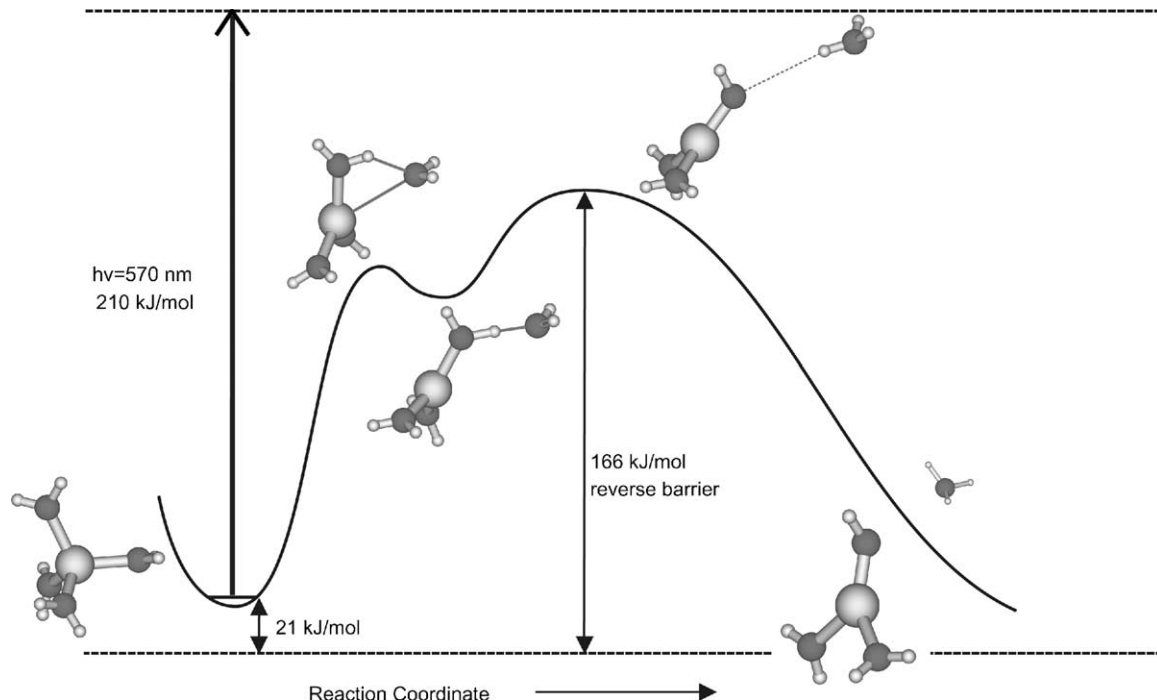
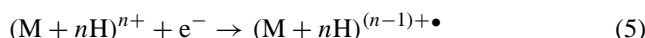


Fig. 8. Reaction path for the photodissociation of $\text{Co}^{2+}(\text{H}_2\text{O})_4$ to $\text{CoOH}(\text{H}_2\text{O})_2^+$ and H_3O^+ . A 570 nm photon deposits 210 kJ/mol in $\text{Co}^{2+}(\text{H}_2\text{O})_4$ as electronic excitation. Rapid internal conversion results in a highly vibrationally excited molecular ion. In the first step towards charge separation, one water ligand moves to the second solvation shell. Subsequently, a proton is transferred from a water molecule in the first solvation shell to one in the second solvation shell, followed by Coulombic explosion of the complex. Of the ~ 231 kJ/mol available energy, 110 ± 20 kJ/mol is released as kinetic energy.

cause it to behave quite differently from the solvated analogue. The photodissociation spectrum of $\text{Co}^{2+}(\text{CH}_3\text{OH})_6$ (Fig. 5) has a peak cross-section of $\sigma \approx 2.8 \times 10^{-19} \text{ cm}^2$, a factor of four larger than that of $\text{Co}^{2+}(\text{H}_2\text{O})_6$. In solution, methanolic cobalt(II) only absorbs about 40% more strongly than aqueous cobalt(II). One possible explanation is that the bulkier ligands cause the complex to distort further from octahedral geometry, and that this distortion is more pronounced in the gas-phase cluster. This is supported by solution spectra of cobalt(II) in larger alcohols: spectra in *iso*-propanol and *tert*-butanol are significantly different from those in water and methanol, while ethanolic solutions are intermediate and temperature-dependent. We are exploring this further in gas-phase studies of Co^{2+} complexes with larger alcohols.

3.3. Spectroscopy of multiply charged proteins

Proteins are sufficiently large that they can support multiple charged sites that do not interact strongly. How the extent of protonation and the solvent affects protein tertiary structure is an area of active inquiry, and one which spectroscopy of gas-phase ions is just beginning to address. Infrared multiphoton dissociation (IRMPD) has been used to help determine the tertiary structure of gas-phase protein ions. Typically, electron capture dissociation (ECD) is used to break a covalent bond in the backbone of an n -protonated protein:



The protein may still be held together by tertiary, noncovalent bonding. IRMPD of $(\text{M} + n\text{H})^{(n-1)+}\bullet$ then produces characteristic fragments. McLafferty and coworkers [35] have extended this technique by measuring the IR photodissociation spectrum of the $(\text{M} + 7\text{H})^{6+}\bullet$ and $(\text{M} + 8\text{H})^{7+}\bullet$ ions of ubiquitin from 3050 to 3800 cm^{-1} . They observe a broad peak at 3350 cm^{-1} that is likely due to the N-H stretch of hydrogen-bonded protonated amine residues.

Andersen et al. demonstrated some of the potential of combining an ESI ion source with an electrostatic heavy-ion storage ring by photodissociating $[\text{cytochrome } c + 17\text{H}]^{17+}$ at 532 nm [99]. Fuke and coworkers have also irradiated $[\text{cytochrome } c + n\text{H}]^{n+}$ ($n = 9-17$) at 532 and 355 nm. Rather than photodissociation, they observe photoionization to form $[\text{cytochrome } c + n\text{H}]^{(n+1)+}$ via a two-photon process, with the ionization yield decreasing rapidly for the more highly charged ions. This is consistent with a model in which the highly charged protein is completely unfolded, forming a linear polypeptide chain [48].

3.4. Multiply charged metal cluster ions

Several groups have studied the stability and collision induced dissociation of cluster ions M_n^{z+} formed by photoionization. Martin et al. have extended these studies by producing Na_n^{z+} ($z = 7$ and n up to several hundred) by 193 nm photoionization of neutral clusters [100]. The cluster ions were then “heated” by irradiating them at 470 nm, near the plasmon resonance, which leads to evaporation of neutral

and charged fragments. From the resulting mass spectrum they measured the smallest n for a given charge z . The critical condition for stability is given by

$$\frac{z^2}{n} \leq 0.125 \quad (6)$$

A simple, classical liquid droplet model shows that energized clusters dissociate in an asymmetric fashion, losing small, singly charged ions (e.g., Na_{320}^{6+} loses Na_3^+) [101,102]. This is surprisingly similar to the Iribarne–Thomson mechanism for ion production [28] in electrospray ionization.

Schweikhard and coworkers have studied the photodissociation dynamics of metal cluster dianions Au_n^{2-} in an ICR ion trap. Following photoexcitation at 355 nm, they observe two channels: photodetachment (to Au_n^-) and dissociation by loss of one neutral gold atom. Both channels have similar yields for $n = 50$, but photodetachment dominates for smaller clusters ($n \leq 35$). This agrees with cluster models that predict little change of the dissociation energy with cluster size, but that the binding energy of the second electron is smaller for smaller clusters [103,104].

4. Future directions

Studies to date have revealed fascinating spectroscopy and dynamics in multiply charged ions. Because spectroscopy of multiply charged ions, especially those containing more than a handful of atoms, is such a young field, current studies have only begun to reveal the possibilities. There are many promising new techniques and new systems. Laser ablation sources and liquid–nitrogen cooled traps (both discussed in Section 2.1) are welcome steps towards the goal of a general technique that produces intense beams of cold (<20 K) solvated, multiply charged ions. Most spectroscopy of multiply charged ions has relied on photofragmentation following electronic excitation. An exciting recent development is the application of alternative optical techniques such as fluorescence and fluorescence resonance energy transfer (FRET) to explore conformational changes and the effect of hydration on biological molecules in the gas-phase, in ion traps [44,105]. Although the particular ions studied were singly charged, these techniques could also be applied to multiply charged ions.

Infrared spectroscopy of singly charged ions has revealed a great deal about structure and bonding in solvated molecular cations [106–108] and anions [107,109], as the vibrational spectrum is very sensitive to hydrogen bonding and inner versus outer shell solvation. Unlike the case of thermodynamically unstable DCl^{2+} , where vibrational excitation leads to rapid predissociation (Section 3.1), bond strengths in solvated, multiply charged ions typically correspond to several vibrational quanta. Techniques that can overcome this difficulty include infrared multiphoton dissociation (IRMPD), selective electronic photodissociation of vibrationally excited molecules (vibrationally mediated

photodissociation), and photodissociation of molecules “tagged” with a weakly bound spectator (typically argon). These techniques have been extensively applied to neutrals and singly charged ions [108,110–112], and multiply charged ions are a logical target. Along these lines, we are currently evaluating vibrational spectroscopy of solvated transition metal dication using IRMPD.

Acknowledgements

Spectroscopy of multiply charged ions in my group has been carried out by a very talented group of students: Chris Thompson, Fernando Aguirre, Kieron Faherty, Kay Stringer, Jennifer LaForest and Manori Gunawardhana. I am also grateful for valuable theoretical help, and a version of Fig. 8 from Dr. Martin K. Beyer (Technische Universität München) and financial support from the Petroleum Research Fund of the ACS and the National Science Foundation.

References

- [1] J.J. Thomson, *Rays of Positive Electricity*, Longmans, Green, London, 1921.
- [2] M.A. Duncan, *Int. J. Mass Spectrom.* 200 (2000) 545.
- [3] L.M. Roth, B.S. Freiser, *Mass Spectrom. Rev.* 10 (1991) 303.
- [4] J.C. Weisshaar, *Acc. Chem. Res.* 26 (1993) 213.
- [5] D. Schröder, H. Schwarz, *J. Phys. Chem. A* 103 (1999) 7385.
- [6] S.D. Price, *Phys. Chem. Chem. Phys.* 5 (2003) 1717.
- [7] A. Dreuw, L.S. Cederbaum, *Chem. Rev.* 102 (2002) 181.
- [8] X.B. Wang, X. Yang, L.S. Wang, *Int. Rev. Phys. Chem.* 21 (2002) 473.
- [9] L.S. Wang, C.F. Ding, X.B. Wang, S.E. Barlow, *Rev. Sci. Instrum.* 70 (1999) 1957.
- [10] X.B. Wang, L.S. Wang, *J. Phys. Chem. A* 104 (2000) 4429.
- [11] K.G. Spears, G.C. Fesenfeld, M. McFarland, E.E. Ferguson, *J. Chem. Phys.* 56 (1972) 2562.
- [12] R. Tonkyn, J.C. Weisshaar, *J. Am. Chem. Soc.* 108 (1986) 7128.
- [13] K.G. Spears, F.C. Fesenfeld, *J. Chem. Phys.* 56 (1972) 5698.
- [14] M. Beyer, E.R. Williams, V.E. Bondybey, *J. Am. Chem. Soc.* 121 (1999) 1565.
- [15] M. Peschke, A.T. Blades, P. Kebarle, *Int. J. Mass Spectrom.* 187 (1999) 685.
- [16] C.A. Woodward, M.P. Dobson, A.J. Stace, *J. Phys. Chem. A* 101 (1997) 2279.
- [17] A.J. Stace, N.R. Walker, S. Firth, *J. Am. Chem. Soc.* 119 (1997) 10239.
- [18] N.R. Walker, R.R. Wright, P.E. Barran, H. Cox, A.J. Stace, *J. Chem. Phys.* 114 (2001) 5562.
- [19] R.R. Wright, N.R. Walker, S. Firth, A.J. Stace, *J. Phys. Chem. A* 105 (2001) 54.
- [20] M. Velegrakis, C. Luder, *Chem. Phys. Lett.* 223 (1994) 139.
- [21] N.R. Walker, G.A. Grieves, J.B. Jaeger, R.S. Walters, M.A. Duncan, *Int. J. Mass Spectrom.* 228 (2003) 285.
- [22] M. Yamashita, J.B. Fenn, *J. Phys. Chem.* 88 (1984) 4451.
- [23] A.T. Blades, P. Jayaweera, M.G. Ikonomou, P. Kebarle, *J. Chem. Phys.* 92 (1990) 5900.
- [24] A.T. Blades, P. Jayaweera, M.G. Ikonomou, P. Kebarle, *Int. J. Mass Spectrom. Ion Proc.* 102 (1990) 251.
- [25] T.D. Burns, T.G. Spence, M.A. Mooney, L.A. Posey, *Chem. Phys. Lett.* 258 (1996) 669.

- [26] T.G. Spence, T.D. Burns, L.A. Posey, *J. Phys. Chem. A* 101 (1997) 139.
- [27] T.G. Spence, T.D. Burns, G.B. Guckenberger, L.A. Posey, *J. Phys. Chem. A* 101 (1997) 1081.
- [28] J.V. Iribarne, B.A. Thomson, *J. Chem. Phys.* 64 (1976) 2287.
- [29] P. Kebarle, L. Tang, *Anal. Chem.* 65 (1993) 972A.
- [30] P. Kebarle, Y. Ho, in: R.B. Cole (Ed.), *Electrospray Ionization Mass Spectrometry: Fundamentals, Instrumentation and Applications*, Wiley, New York, 1997, p. 3.
- [31] J.N. Smith, R.C. Flagan, J.L. Beauchamp, *J. Phys. Chem. A* 106 (2002) 9957.
- [32] J.B. Fenn, *Int. J. Mass Spectrom.* 200 (2000) 459.
- [33] Y.A. Ranasinghe, T.J. MacMahon, B.S. Freiser, *J. Am. Chem. Soc.* 114 (1992) 9112.
- [34] R.C. Dunbar, *Int. J. Mass Spectrom.* 200 (2000) 571.
- [35] H. Oh, K. Breuker, S.K. Sze, Y. Ge, B.K. Carpenter, F.W. McLafferty, *Proc. Natl. Acad. Sci. U.S.A.* 99 (2002) 15863.
- [36] C.J. Thompson, J. Husband, F. Aguirre, R.B. Metz, *J. Phys. Chem. A* 104 (2000) 8155.
- [37] K.P. Faherty, C.J. Thompson, F. Aguirre, J. Michne, R.B. Metz, *J. Phys. Chem. A* 105 (2001) 10054.
- [38] S.K. Chowdhury, V. Katta, B.T. Chait, *J. Rapid Commun. Mass Spectrom.* 4 (1990) 81.
- [39] L. Drahos, R.M.A. Heeren, C. Collette, E. De Pauw, K. Vékey, *J. Mass Spectrom.* 34 (1999) 1373.
- [40] A.A. Shvartsburg, *J. Am. Chem. Soc.* 124 (2002) 12343; A.A. Shvartsburg, *Chem. Phys. Lett.* 360 (2002) 479.
- [41] A.M. El-Nahas, N. Tajima, K. Hirao, *Chem. Phys. Lett.* 318 (2000) 333; A.A. Shvartsburg, K.W.M. Siu, *J. Am. Chem. Soc.* 123 (2001) 10071; J.A. Stone, D. Vukomanovic, *Chem. Phys. Lett.* 346 (2001) 419; D. Schröder, H. Schwarz, J. Wu, C. Wesdemiotis, *Chem. Phys. Lett.* 343 (2001) 258.
- [42] B.M. Chien, S.M. Michael, D.M. Lubman, *Int. J. Mass Spectrom. Ion Proc.* 131 (1994) 149.
- [43] C.-F. Ding, X.-B. Wang, L.-S. Wang, *J. Phys. Chem. A* 102 (1998) 8633.
- [44] J.T. Khoury, S.E. Rodriguez-Cruz, J.H. Parks, *J. Am. Soc. Mass Spectrom.* 13 (2002) 696.
- [45] S. Schlemmer, A. Luca, J. Glosik, D. Gerlich, *J. Chem. Phys.* 116 (2002) 4508.
- [46] L.A. Posey, M.J. DeLuca, M.A. Johnson, *Chem. Phys. Lett.* 131 (1986) 170.
- [47] P.C. Cosby, R. Moller, H. Helm, *Phys. Rev. A* 28 (1983) 766.
- [48] S. Nonose, S. Iwaoka, H. Tanaka, N. Okai, T. Shibakusa, K. Fuke, *Eur. Phys. J. D24* (2003) 335.
- [49] L.N. Ding, P.D. Kleiber, M.A. Young, W.C. Stwalley, A.M. Lyrya, *Phys. Rev. A* 48 (1993) 2024.
- [50] M.K. Beyer, R.B. Metz, *J. Phys. Chem. A* 107 (2003) 1760.
- [51] S.G. Cox, A.D.J. Critchley, P.S. Kreynin, I.R. McNab, R.C. Shiell, F.E. Smith, *Phys. Chem. Chem. Phys.* 5 (2003) 663.
- [52] S.D. Price, *J. Chem. Soc., Faraday Trans.* 93 (1997) 2451.
- [53] J. Senekowitsch, S. O'Neil, P. Knowles, H.-J. Werner, *J. Phys. Chem.* 95 (1991) 2125.
- [54] A.S. Mullin, D.M. Szaflarski, K. Yokoyama, G. Gerber, W.C. Lineberger, *J. Chem. Phys.* 96 (1992) 3636.
- [55] P.K. Carroll, *Can. J. Phys.* 36 (1958) 1585.
- [56] D. Cossart, F. Launay, J.M. Robbe, G. Gandara, *J. Mol. Spectrosc.* 113 (1985) 142.
- [57] D. Cossart, F. Launay, *J. Mol. Spectrosc.* 113 (1985) 159.
- [58] T.E. Masters, P.J. Sarre, *J. Chem. Soc., Faraday Trans.* 86 (1990) 2005.
- [59] M. Larsson, *Comments At. Mol. Phys.* 29 (1993) 39.
- [60] D. Cossart, M. Bonneau, J.M. Robbe, *J. Mol. Spectrosc.* 125 (1987) 413.
- [61] D. Cossart, C. Cossart-Magos, *J. Mol. Spectrosc.* 147 (1991) 471.
- [62] L.G.M. Pettersson, L. Karlsson, M.P. Keane, A.N. Debrito, N. Correia, M. Larsson, L. Brostrom, S. Mannervik, S. Svensson, *J. Chem. Phys.* 96 (1992) 4884.
- [63] R. Abusen, F.R. Bennett, I.R. McNab, D.N. Sharp, R.C. Shiell, G.A. Woodward, *J. Chem. Phys.* 108 (1998) 1761.
- [64] R. Abusen, F.R. Bennett, S.G. Cox, I.R. McNab, D.N. Sharp, R.C. Shiell, F.E. Smith, J.M. Walley, *Phys. Rev. A* 6105 (2000).
- [65] Y.Y. Lee, S.R. Leone, P. Champkin, N. Kaltsouyannis, S.D. Price, *J. Chem. Phys.* 106 (1997) 7981.
- [66] Y.Y. Lee, S.R. Leone, *J. Phys. Chem.* 99 (1995) 15438.
- [67] S.D. Price, Y.Y. Lee, M. Manning, S.R. Leone, *Chem. Phys.* 190 (1995) 123.
- [68] T.G. Spence, B.T. Trotter, L.A. Posey, *Int. J. Mass Spectrom.* 177 (1998) 187.
- [69] M. Kohler, J.A. Leary, *Int. J. Mass Spectrom. Ion Proc.* 162 (1997) 17.
- [70] M. Kohler, J.A. Leary, *J. Am. Soc. Mass Spectrom.* 8 (1997) 1124.
- [71] A.J. Stace, *Phys. Chem. Chem. Phys.* 3 (2001) 1935.
- [72] A.J. Stace, *J. Phys. Chem. A* 106 (2002) 7993.
- [73] W.E. Rodriguez-Cruz, R.A. Jockusch, E.R. Williams, *J. Am. Chem. Soc.* 120 (1998) 5842.
- [74] A.A. Shvartsburg, J.G. Wilkes, J.O. Lay, K.W.M. Siu, *Chem. Phys. Lett.* 350 (2001) 216.
- [75] A.A. Shvartsburg, J.G. Wilkes, *J. Phys. Chem. A* 106 (2002) 4543.
- [76] M.Y. Combariza, R.W. Vachet, *J. Phys. Chem. A* 108 (2004) 1757.
- [77] N.G. Tsierkezos, D. Schröder, H. Schwarz, *J. Phys. Chem. A* 107 (2003) 9575.
- [78] T.G. Spence, B.T. Trotter, T.D. Burns, L.A. Posey, *J. Phys. Chem. A* 102 (1998) 6101.
- [79] T.G. Spence, B.T. Trotter, L.A. Posey, *J. Phys. Chem. A* 102 (1998) 7779.
- [80] L.A. Posey, in: M.A. Duncan (Ed.), *Advances in Metal and Semiconductor Clusters*, Elsevier, New York, 2001, p. 145.
- [81] L. Puskar, A.J. Stace, *J. Chem. Phys.* 114 (2001) 6499.
- [82] L. Puskar, H. Cox, A. Goren, G.D.C. Aitken, A.J. Stace, *Faraday Discuss.* 124 (2003) 259.
- [83] L. Puskar, P.E. Barran, R.R. Wright, D.A. Kirkwood, A.J. Stace, *J. Chem. Phys.* 112 (2000) 7751.
- [84] J. Friedrich, S. Gilb, O.T. Ehrler, A. Behrendt, M.M. Kappes, *J. Chem. Phys.* 117 (2002) 2635.
- [85] H. Ohtaki, T. Radnai, *Chem. Rev.* 93 (1993) 1157.
- [86] D. Sutton, *Electronic Spectra of Transition Metal Complexes*, McGraw-Hill, London, 1968.
- [87] A.B.P. Lever, *Inorganic Electronic Spectroscopy*, second ed., Elsevier, Amsterdam, 1984.
- [88] F.A. Cotton, G.W. Wilkinson, *Advanced Inorganic Chemistry*, Wiley, London, 1988.
- [89] H.S.R. Gilson, M. Krauss, *J. Phys. Chem. A* 102 (1998) 6525.
- [90] H.S.R. Gilson, M. Krauss, *J. Phys. Chem. A* 104 (2000) 5653.
- [91] T.W. Swaddle, L. Fabes, *Can. J. Chem.* 58 (1980) 1418.
- [92] C. Fedorchuk, T.W. Swaddle, *J. Phys. Chem. A* 104 (2000) 5651.
- [93] R.B. Metz, *Int. Rev. Phys. Chem.* 23 (2004) 79.
- [94] H. Köppel, W. Domcke, L. Cederbaum, *Adv. Chem. Phys.* 57 (1984) 59.
- [95] A.B. Rocha, C.E. Bielschowsky, *Chem. Phys.* 253 (2000) 51.
- [96] I. Borges Jr., A.J.C. Varandas, A.B. Rocha, C.E. Bielschowsky, *J. Mol. Struct. (Theochem.)* 621 (2003) 99.
- [97] F. Aguirre, J. Husband, C.J. Thompson, K.L. Stringer, R.B. Metz, *J. Chem. Phys.* 119 (2003) 10194.
- [98] T. Borowski, E. Broclawik, *Chem. Phys. Lett.* 339 (2001) 433.
- [99] J.U. Andersen, P. Hvelplund, S.B. Nielsen, S. Tomita, H. Wahlgreen, S.P. Moller, U.V. Pedersen, J.S. Forster, T.J.D. Jorgensen, *Rev. Sci. Instrum.* 73 (2002) 1284.
- [100] T.P. Martin, U. Naher, H. Gohlich, T. Lange, *Chem. Phys. Lett.* 196 (1992) 113.
- [101] U. Naher, S. Frank, N. Malinowski, U. Zimmermann, T.P. Martin, *Z. Phys. D: Atoms Mol. Clusters* 31 (1994) 191.

- [102] U. Naher, S. Bjornholm, S. Frauendorf, F. Garcias, C. Guet, Phys. Rep.-Rev. Sec. Phys. Lett. 285 (1997) 245.
- [103] L. Schweikhard, K. Hansen, A. Herlert, M.D.H. Lablanca, G. Marx, M. Vogel, Int. J. Mass Spectrom. 219 (2002) 363.
- [104] L. Schweikhard, K. Hansen, A. Herlert, M.D.H. Lablanca, G. Marx, M. Vogel, Hyperfine Interact. 146 (2003) 275.
- [105] A.S. Danell, J.H. Parks, Int. J. Mass Spectrom. 229 (2003) 35.
- [106] J.M. Lisy, Int. Rev. Phys. Chem. 16 (1997) 267.
- [107] E.J. Bieske, O. Dopfer, Chem. Rev. 100 (2000) 3963.
- [108] M.A. Duncan, Int. Rev. Phys. Chem. 22 (2003) 407.
- [109] W.H. Robertson, E.A. Price, J.M. Weber, J.-W. Shin, G.H. Weddle, M.A. Johnson, J. Phys. Chem. A 107 (2003) 6527.
- [110] M. Okumura, L.I. Yeh, J.D. Meyers, Y.T. Lee, J. Chem. Phys. 85 (1986) 2328.
- [111] P. Ayotte, C.G. Bailey, J. Kim, M.A. Johnson, J. Chem. Phys. 108 (1998) 444.
- [112] F.F. Crim, Annu. Rev. Phys. Chem. 44 (1993) 397.